EES Solar

PAPER

View Article Online
View Journal | View Issue

Cite this: *EES Sol.*, 2025, **1**, 536

Photocatalyst sheet performance under intense UV irradiation and increased temperatures†

Talib M. Rahman, [a] D. J. Osborn, III,[a] Anthony E. Pellicone, [a] Patrick C. Tapping, [a] Tsuyoshi Takata,[b] Takashi Hisatomi, [b] Hiroshi Nishiyama,[c] Kazunari Domen, [c] Gunther G. Andersson [d] and Gregory F. Metha *[a]

Immobilised nano-particulate photocatalyst sheets offer a simplified approach to scaling water-splitting photocatalytic systems for low-emission hydrogen production. This work investigated the effect of increased UV irradiation and temperature on the water-splitting performance of CoOOH/$RhCrO_x$/$SrTiO_3$:Al photocatalyst sheets. UV photon fluxes from 1.75×10^{19} to over 250×10^{19} photons per cm^2 per h were investigated at ambient temperature (23 °C). Although the water-splitting rate increased with increasing intensity, the apparent quantum yield (AQY) was observed to decrease. The effect of temperature on liquid water splitting at 23 °C, 35 °C, 50 °C, 90 °C and 120 °C was further explored upon increasing UV photon flux. It was found that increasing temperatures improve the AQY relative to the photon fluence. The reason for this effect is discussed in terms of bulk and surface effects reducing recombination. A method to equate light sources to solar equivalents was developed and used to relate the UV photon fluxes investigated to concentrated solar equivalents. This work demonstrates the use of heating to improve the efficiency of photocatalytic water splitting, draws attention to the necessity for considering the incident absorbable light intensity in measuring the performance of photocatalysts, and highlights the potential application of photocatalyst sheets under concentrated solar conditions.

Received 11th April 2025
Accepted 7th May 2025

DOI: 10.1039/d5el00059a

rsc.li/EESSolar

Broader context

Overall water-splitting *via* photocatalysis offers a method to produce low-emission hydrogen, if powered by solar energy. However, this technology is not currently competitive to conventional electrolysis as it is constrained by low overall system efficiencies. While the field progresses to develop photocatalysts with competitive efficiencies, it is crucial to develop a reactor technology for this material to be situated in. Immobilised nano-particulate photocatalyst sheets offer a simplified approach to scaling water-splitting photocatalytic systems; however, these materials often rely on precious metals. Concentrated solar systems would allow for a reduction in the required quantity of the photocatalyst and have additional benefits as photocatalyst performance is increased by heating. This study aims to investigate the performance of photocatalyst sheets at increased light intensities and temperatures to inform the design of a concentrated system.

Introduction

Since the demonstration of the Honda–Fujishima effect in 1972,[1] over 50 years of research has taken place to investigate the use of photocatalysis for water-splitting. Solar powered photocatalysts can be utilised to produce low emission hydrogen, as this process is only dependent on sunlight and water, with a co-product of oxygen.

Overall solar driven water-splitting *via* particulate photocatalysts offers a straightforward approach to produce hydrogen, with both light absorption and catalysis taking place on single particles.[2] An example of such a system has been demonstrated by Nishiyama *et al.* with a 100 m^2 panel system using photocatalyst sheets.[3] By immobilising the photocatalyst sheets, difficulties with upscaling photocatalyst systems are overcome, such as reducing the weight of the system by reducing the required water volumes, removing energy requirements necessary to keep the particles in suspension *via* forced mixing, and removing the need to recover the suspended particles.[4] Although this work demonstrates a functional solar driven photoreactor, it is currently limited by the low solar-to-hydrogen (STH) efficiency of available photocatalysts, reaching a maximum STH of approximately 0.76%.[3]

Photocatalyst systems are currently not competitive with alternative low-emission hydrogen production technologies, such as electrolysis, as they are limited by low STH efficiency,

[a]*Department of Chemistry, School of Physics, Chemistry and Earth Sciences, University of Adelaide, Australia. E-mail: greg.metha@adelaide.edu.au*

[b]*Research Initiative for Supra-Materials (RISM), Shinshu University, Japan*

[c]*Office of University Professors, The University of Tokyo, Japan*

[d]*Flinders Institute for NanoScale Science and Technology, Flinders University, Australia*

† Electronic supplementary information (ESI) available. See DOI: https://doi.org/10.1039/d5el00059a

which is constrained by both the bandgap and the quantum efficiency of the photocatalyst.[2] The STH efficiency of a photocatalyst is considered to be the most influential factor in producing cost competitive hydrogen under solar conditions, and thus for this technology to become cost competitive, photocatalysts with an improved STH of between 5 and 10% must be engineered.[4,5]

Due to the inherent minimum energy required for water splitting of 1.23 eV ($\lambda = 1008$ nm), regardless of the progress towards visible light responsive photocatalysts, there will always be a significant portion of the solar spectrum that cannot be used directly for single-step solar driven water-splitting.[2,6,7] With STH targets of 10% required for an economically viable system, the portion of the incident energy to the photo-reactor not directly consumed by the water-splitting process can be significant.[5] To increase the efficiencies of solar photoreactors, energy outside of the bandgap must be harvested. An example of energy harvesting for photocatalysts is the work of Kageshima *et al.* By introducing defect states to TiO_2, photothermal effects induced by visible light absorption at defect sites were shown to lead to increased surface temperatures, which improved the hydrogen evolution.[8]

Photocatalytic rate can be positively influenced by an increase in temperature. For metal oxide photocatalysts, studies into the temperature dependence of the bandgap indicate a redshift with increasing temperatures.[9,10] This redshift allows for increased absorption of the solar spectrum and thus an expected increase in STH at increased temperatures. Under simulated solar conditions, Goto *et al.* showcased an increase in STH from 0.4% to 0.6% when the temperature is increased from 15 °C to 58 °C for $RhCrO_x$/Al:$SrTiO_3$ photocatalyst suspensions.[11] For TiO_2 nanoparticles and nanotubes, Peh *et al.* recorded a rate increase of 20- and 40-fold, respectively, when increasing the temperature from 25 to 90 °C.[12] Castedo *et al.* reported that under single wavelength conditions, an increase in temperature from 25 °C to 85 °C under a constant UVA intensity of 1.5 mW cm^{-2} led to a 6-fold increase in rate for Au:TiO_2 using ethanol as a sacrificial reagent.[13] The studies investigating $RhCrO_x$/Al:$SrTiO_3$ and Au:TiO_2 both indicate an Arrhenius relationship.

While improvements in STH seen by Goto *et al.* could be attributed to temperature-related absorption increases, the substantial increases in rate shown by Peh *et al.*, and rate improvements under a single wavelength source by Castedo and colleagues suggest non-absorption-related mechanisms driving the improved performance.

Increasing temperatures have also been reported to increase the STH of Rh/Cr_2O_3/Co_3O_4 loaded indium gallium nitride nanowire (InGaN/GaN NW) photocatalysts from under 0.5% to up to 9% when increasing the temperature from 30 °C to 70 °C, respectively, under simulated concentrated solar light (3800 mW cm^{-2}).[14] Although this study showed a high STH with increasing temperature, it also indicated that beyond 70 °C the STH no longer increased. Zhou *et al.* contended that the rate no longer increases due to enhanced recombination of hydrogen and oxygen beyond 70 °C.[14]

Investigation into photocatalyst reaction rates beyond 100 °C is limited. The performance of N-doped TiO_2 for overall water splitting between temperatures of 200 and 300 °C has been shown to be highly dependent on applied temperatures.[15] The relationship between the temperature and rate shown by Li and colleagues does not increase linearly, with a maximum reached near 270 °C and a decline beyond this temperature.[15] Li and colleagues related the relationship between rate and temperature to the auto-ionisation constant of water, as hydronium and hydroxide ions are more readily reduced than H_2O.[2,15,16]

Under standard solar conditions, it is unlikely that a system will reach the elevated temperatures required to have a significant influence on production rates. To increase the available energy incident on the photocatalyst system, (photoreactor) concentrating systems may be used. Concentrated solar power (CSP) systems take advantage of mirrors or lenses to concentrate sunlight onto a much smaller area. Such systems are conventionally used for heating applications, such as heliostats and linear Fresnel reflectors, but could be leveraged for photocatalyst systems. The cost sensitivity of hydrogen production for photoelectrochemical (PEC) systems has been modelled by Pinaud and colleagues, where their study suggested that the use of concentrating systems could allow for a reduced cost of hydrogen and a reduced sensitivity to the cost of the photocatalyst; however, further technoeconomic modelling would be required for each individual system.[5]

With increasing solar concentration, a photoreactor will receive an elevated number of photons. The influence of light intensity on the photocatalytic rate has been shown extensively in the literature to follow three operating regions with increasing light intensities: the linear, sub-linear, and zero-order regions.[17–20] The transition to the sub-linear region occurs due to physical processes.[17,21] Beyond certain light intensities, the rate at which charge carriers are produced exceeds the rate at which they can be consumed by redox reactions. This leads to an accumulation of charge carriers in the bulk of the photocatalyst particles. As recombination is a second order reaction with respect to charge carrier concentration, the increasing accumulation at increasing light intensities leads to increasing rates of recombination, leading to the sub-linear region and finally the zero-order region.[17,22] In the zero-order region, all surface sites are considered active, and thus the rate is constrained entirely by the kinetics of the reaction.[23] The light intensity at which the reaction rate transitions from linear to sub-linear is intrinsic to the material. This transition is dependent on both bulk and surface processes, which have been improved through examples such as decreasing defect density, increasing availability of reactants, and co-catalyst loading.[7] A material that exhibits such improvements was reported by Takata *et al.*; $SrTiO_3$:Al with a photodeposited Rh/Cr_2O_3 hydrogen evolution reaction (HER) co-catalyst and a CoOOH oxygen evolution reaction (OER) co-catalyst exhibits an external quantum efficiency (EQE) of up to 96%.[24] This material utilises Al doping to reduce defects, a Cr_2O_3 overlayer to prevent the back-reaction by blocking access of O_2 to the Rh co-catalyst, and photo-deposition of the co-catalysts to specific crystal facets to which the photoexcited electrons and holes migrate.[11,25]

Although literature indicates that increasing temperatures lead to increasing production rates for particulate systems, it is not in agreement with the drivers of increasing production rate,

nor does it consider the relationship between temperature and elevated light intensities on the production rate.[2,11–16] This work investigates the relationship between light intensity, temperature, and production rate for photocatalyst sheets of CoO_y/$RhCrO_x$/Al:$SrTiO_3$ ("the photocatalyst"). By using a high-powered single wavelength UV LED array (365 nm) as the source of light, absorbance related improvements in the performance of the photocatalyst can be disregarded, as 365 nm is in the deeply absorbing region of Al:$SrTiO_3$,[24] and high incident absorbable light intensities at the photocatalyst can be reached beyond that achievable using a standard solar simulator. Using UV-visible diffuse reflectance spectroscopy (DRS) measurements of the photocatalyst, a standardisation for solar equivalents is proposed ("Solar Equivalent") and is used to equate the incident UV light intensities within this study to concentrated solar equivalents. Light intensities up to 300 solar equivalents and temperatures up to 120 °C are investigated.

Experimental procedures

Photocatalyst sheet preparation

Photocatalyst samples of $SrTiO_3$:Al with co-catalysts $RhCrO_x$ (Rh 0.1 wt% and Cr 0.1 wt%) and CoO_y (0.1 wt%) were fabricated into photocatalyst sheets through spray coating using methods described by Goto *et al.*[11] The photocatalyst particles were embedded in a sheet layer and adhered to a glass substrate using SiO_2 nanoparticles (diameter, *ca.* 20 nm) and $CaCl_2$ as an inorganic binder. Fabrication of 25 cm^2 samples investigated herein was done at the University of Tokyo and sent to the University of Adelaide for testing, in accordance with procedures previously reported by Nishiyama and Goto.[3,11]

Thermo-photocatalytic reactor

All data were collected using a thermo photo-reactor setup that allows for controlled heating and illumination of the photocatalyst sheets. This apparatus consists of a reactor cell to house the photocatalyst sheet samples, an insulated oven to house and heat the reactor cell, a high-powered UV LED array, and a eudiometer for gas collection. The reactor cell design is the same as that used by Goto and colleagues at the University of Tokyo.[11]

The reactor cell houses 5 × 5 cm photocatalyst sheet samples and comprises a centre piece sandwiched between the window frame and the backing plate, with one inlet hole for water and two outlet holes to allow for unmitigated gas release from the cell. The centre piece of the reactor cell is machined from a single piece to contain a cavity within which the photocatalyst sheet sample is housed. This centre is sealed by a window between the window frame and the stainless-steel backing plate. Water in the reactor cell cavity is replenished as required to ensure that the photocatalyst sheet sample is fully submerged in water while operating. When operated above 100 °C, liquid water was maintained within the reactor using a back pressure regulator (Equilibar, ZF series), and gas production rate was measured volumetrically using a eudiometer, with all reported rates being an average of at least three repeated measurements. Gas composition at a stoichiometric ratio was measured using a gas chromatograph. Due to limitations with the backpressure regulator, consistent gas release was only possible for production rates beyond 100 μmol cm^{-2} h^{-1}.

The insulated oven contains a heating element that heats the air contained within the oven. The temperature within this oven is controlled by a proportional-integral-derivative (PID) temperature controller and a K-type thermocouple in direct contact with the air within the oven. This control system was developed in line with that previously reported by Alvino and colleagues at the University of Adelaide.[26]

The photocatalyst sheets within the reactor cell were illuminated using a 365 nm LED source (Hamamatsu GJ-75 series). Light intensity was altered through changing the distance between the light source and the reactor and through changing the current applied to the LED array. Incident power was measured using a volume absorbing disc calorimeter (AC2501S, Scientech), with the window included in the path of light to take into account optical losses through the window of the reactor.

Results & discussion

Effect of light intensity

The performance of semiconductors under simulated solar equivalents is often standardised by comparing the optical power output of the simulated solar source to that of a standard solar equivalent, such as the 1000 W m^{-2} of ASTM G-173, AM 1.5G spectrum (Fig. SI-4†). For overall water-splitting *via* photocatalysis, performance is measured by STH, which uses the raw incident solar power as input to the calculation. However, hydrogen production is more realistically dependent on the photocatalyst bandgap and thus the number of incident absorbable photons, rather than simply the total power of the input light source.

Simulated solar sources, such as xenon arc lamps, have some degree of spectral mismatch to that of reference solar spectra, even in the case where specialised optical filters are used to better match the solar spectrum. This mismatch can be significant if the samples irradiated only utilise a limited part of the optical spectrum, such as the UV region. In this case, the equivalent number of absorbable photons in the reference solar spectrum provides a more appropriate benchmark than the raw overall power of the simulated solar source. The performance of a photocatalyst under a simulated solar equivalent requires considering the number of photons present in the broad-spectrum solar standard that are absorbable by the photocatalyst being investigated. To the authors' knowledge, this has not previously been fully addressed in the literature.

Equating concentrated solar equivalents for photocatalyst performance under any light source requires three key data sets:

(1) The absorbance of the photocatalyst as a function of wavelength (absorbance profile).

(2) The spectral power density of the standard solar reference.

(3) The spectral power density of the source of light used in the investigation.

UV-visible DRS measurements of $CoO_y/RhCrO_x/Al:SrTiO_3$ nanoparticles were interpreted to obtain the Kubelka–Munk absorbance of the photocatalyst as a function of photon energy, and it was applied to calculate the solar equivalents from the UV LED array used in this study. The calculated number of absorbable photons available for this photocatalyst is 8.32×10^{18} photons per cm^2 per h (*i.e.* 1 solar equivalent), where the standard solar reference used is ASTM G-173-03 AM 1.5 D (Fig. SI-4,† red trace) as this spectrum most closely matches with concentrated solar conditions, see ESI Section II† for further details.

The performance of the photocatalyst sheet at increasing light intensities was first explored at ambient temperatures (23 °C). As the source of light is a single wavelength source, light intensity measurements can be converted into number of photons or photon flux, *e.g.* 1 W measured from a 365 nm source is approximately equal to 1.84×10^{18} photons and 1.3 mW cm^{-2} is approximately one solar equivalent. The sample was exposed to photon fluxes ranging from 1.75×10^{19} to over 250×10^{19} photons per cm^2 per h, over an 150-fold increase in intensity. As seen in Fig. 2, the observed production rate of hydrogen increases with increasing light intensity for all intensities investigated.

To best visualise the effect of light intensity on the production rate of the sheet, data can be represented in two measures, the rate of production of hydrogen gas (Fig. 1a) and the AQY *versus* photon flux (Fig. 1b), respectively. All production rates are reported in units of μmol cm^{-2} h^{-1}, which includes the area to ensure that any future samples with different surface areas may be directly compared.

As the photon flux increases, the production rate increases non-linearly (Fig. 1a). This relationship is reflected by the AQY calculations for these data points which indicate a steep drop in the initial AQY from around 30% to around 5% (Fig. 1b). This agrees with that described in the literature that there is a non-linear relationship between light intensity and production rate at elevated light intensities.[17,18]

Effect of temperature

Using a reactor oven setup, the influence of temperature on the reaction rate was investigated between 23 and 120 °C for photon fluxes up to around 100×10^{19} photons per cm^2 per h. The relationship of hydrogen production rate with light intensity and temperature is shown in Fig. 2a and follows the general trend previously described in the literature that increased light intensity leads to a sub-linear increase in the production rate beyond a certain intensity and that increased temperature leads to increased production rates.[11–15] As the light intensity increases, the AQY decreases (Fig. 2b). This decreased AQY at elevated light intensities is overcome through increasing temperature. Across the temperature ranges investigated, the greatest improvement in AQY occurs between 50 °C and 90 °C, with the AQY converging to 10% at 50 °C and approximately 20% at 90 °C and 120 °C.

At lower intensities, closer to 1 solar equivalent, an increase in temperature is shown to have negligible influence on the reaction rate, as shown in Fig. 3a. Furthermore, there is a non-linear relationship between the temperature and production rate under the elevated light intensities investigated. To better understand the form of the temperature relationship, Fig. 3a has been transformed into an Arrhenius plot. When presented in this form, the relationship conforms to that expected of an Arrhenius relationship. Using production rate as a proxy for rate constant, the activation energy of each intensity has been calculated using the slope of the corresponding line (as depicted in Fig. 3b and Fig. SI-2b†). This analysis assumes that temperature related changes with respect to reactant concentration are negligible, as the reactant is pure water. At higher intensities, a positive activation energy is noted which increases with increasing light intensity, indicating a greater dependence on temperature under a higher photon flux. This suggests that at elevated light intensities an increase in temperature allows for a rate-determining step to be overcome, the nature of which is unclear. As light intensity continues to increase, the apparent

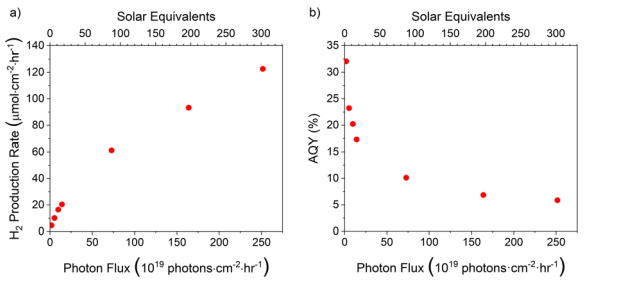

Fig. 1 (a) Hydrogen production rate and (b) AQY of the photocatalyst sheet at an ambient temperature of 23 °C under increasing photon flux.

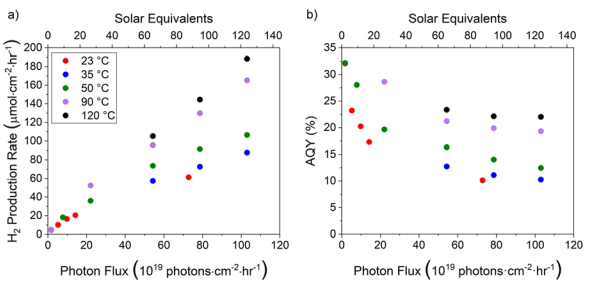

Fig. 2 (a) Hydrogen production rate and (b) AQY of the photocatalyst sheet in the temperature range 23–120 °C.

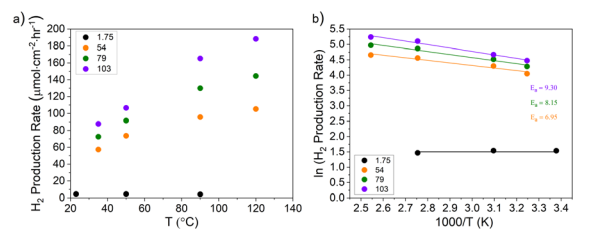

Fig. 3 (a) Hydrogen production rate and (b) natural log of production rate of the photocatalyst sheet at varying photon flux with increasing temperature.

activation energy is predicted to converge.[23] The convergence of activation energy indicates the upper limit of the reaction rate achievable by the photocatalyst and signifies the commencement of the zeroth order region.

As incident light intensities increase, increased charge carrier densities are generated within the nanoparticles. The reduced AQY observed with increasing light intensity occurs due to increased recombination, as recombination is of second order in relation to the charge carrier density. The observed recovery in the AQY with increasing temperatures at elevated light intensities indicates a reduction in recombination, which could be caused by either bulk effects, surface-related effects, or a combination of the two. While the exact mechanism has not been elucidated in this study, we propose the following potential reasons for further investigation.

Bulk-related effects

The increase noted in the AQY could be caused by an improvement in interfacial charge transfer with increasing temperature. At increasing temperatures, electrochemical impedance spectroscopy (EIS) of TiO_2 films show reduced charge transfer resistance.[27–29] This would lead to reduced recombination as the charge carriers are able to transfer into the co-catalyst active sites more readily. Reduced recombination in TiO_2 films due to temperature has been further confirmed by Li *et al.*, who showcased a reduction in photoluminescence (PL) spectra with increased temperature.[29]

Charge carrier extraction rates in nanoparticulate Al:$SrTiO_3$ has been investigated by Muthy *et al.* using time-resolved diffuse reflectance (TDR) and time-resolved microwave conductance (TRMC) spectroscopy.[30] By comparing TDR and TRMC measurements of Al:$SrTiO_3$ with $SrTiO_3$ and doping with a Rh co-catalyst, Muthy *et al.* concluded that the excellent performance of Al:$SrTiO_3$ can be attributed to an electron extraction rate much greater than the carrier-recombination rate, allowing for electrons to be extracted into the Rh co-catalyst active sites before they are able to recombine. While this study is targeted at understanding the influence of Al doping on increased performance of $SrTiO_3$, it explores the importance of the charge carrier extraction rate relative to the carrier-recombination rate. With increasing light intensities, the carrier-recombination rate may exceed that of the extraction rate. As indicated by studies of TiO_2 films, increasing temperatures favour interfacial charge transfer, which would improve the extraction rate, allowing for the extraction rate to increase with respect to the recombination rate thus reducing recombination.

While, to the authors' knowledge, there has been no equivalent work studying charge carrier extraction within nanoparticulates at increasing temperatures, the hypothesized charge carrier improvements could lead to the improved AQY observed in this study.

Surface-related effects

The observed increase in AQY with increasing temperatures at elevated light intensities could be linked to improved surface kinetics. With increasing temperatures, the auto-ionisation of water increases, leading to a greater availability of hydronium (H_3O^+) and hydroxide (OH^-) ions (Fig. SI-3 and Table SI-1†).[31] As OH^- and H^+ are preferentially oxidised and reduced at redox sites over H_2O molecules, an increase in availability of these reactants would allow for the faster consumption of electrons and holes at surface redox sites, increasing charge carrier lifetime by reducing accumulation and thus recombination at higher light intensities.[2,15]

Liu *et al.* further discuss surface related improvements of metal oxide photoanodes with increasing temperatures.[32] In their study, they noted in linear sweep voltammetry experiments, a monotonical improvement in photocurrent density for TiO_2 across all applied potentials with increasing temperature. However, for Fe_2O_3, they noted a negative temperature relationship at low applied potentials and improvements at higher applied potentials. The authors ascribe this difference in improvements to charge trapping in differing rate determining steps (RDS) for each metal oxide at the surface of the photoanode. Liu *et al.* hypothesised that surface charges (holes) are trapped as chemical species at the surface during the water-splitting process and that the RDS for TiO_2 is later in the catalytic cycle and may be limited by thermal steps. Other potential influencing factors on the production rate could be Arrhenius related improvements, and the change in Gibbs free energy of water splitting with increasing temperature. Across the range of temperatures investigated, the Gibbs free energy of liquid water splitting decreases, indicating more favorable kinetics (see ESI Section III† for more details).

An alternative method through which recombination may be reduced is by increasing the concentration of co-catalyst deposited. Hisatomi and colleagues investigated the effect of light intensity and co-catalyst loading on $(Ga_{1-x}Zn_x)(N_{1-x}O_x)$ and found that the optimum loading of co-catalyst is dependent on the operating light intensity.[17] The photocatalyst sheets investigated were optimised to operate under standard solar conditions and not the elevated photon fluxes in this study. Further investigation into the influence of co-catalyst loadings at elevated temperatures and photon flux is required to understand potential improvements through increased loadings.

Conclusions

This work demonstrates the performance of photocatalyst sheets at elevated UV intensities and increasing temperatures. A method to equate light sources to reference solar equivalents is presented and applied to the 365 nm LED array used in this study. This equivalency is a useful tool to benchmark incident photon flux to solar conditions, an overlooked aspect of testing photocatalyst performance. By equating the UV intensity to solar equivalents, it is apparent that increased absorbable light intensities from solar concentration will lead to lower system efficiencies. However, these efficiency losses can be overcome by increasing the temperature, which will likely be realisable under concentrated solar conditions as the photocatalyst will simultaneously receive increased incident energy from outside of the

bandgap, showcasing the potential for the use of these sheets under concentrated solar conditions.

It is hypothesised that the increase in AQY with increasing temperature is caused by overcoming recombination; however, the underlying effect is not yet understood. Due to design constraints of the reactor used, temperatures above 120 °C have not yet been investigated for these sheets. Future investigation should look to assess the influence of surface related effects, by increasing the operating temperature of the reactor to the maximum auto-ionisation constant of water of around 250 °C,[31] assessing the influence of increased loadings of co-catalysts and further investigating the activation energy at lower solar concentrations.

Data availability

The data supporting this article have been included as part of the ESI.†

Author contributions

T. M. R. performed the photocatalytic reactions. T. T., T. H., H. N., and K. D. produced the photocatalyst samples. D. J. O. designed and constructed the photocatalyst reactor setup. A. E. P. performed the Gibbs free energy calculations. P. C. T. performed the sun equivalent calculations. G. F. M. and G. G. A. supervised the project. T. R. and G. M. wrote the manuscript with input from all authors.

Conflicts of interest

Intellectual properties related to this work have been licensed to Sparc Hydrogen, a joint venture between Sparc Technologies, Fortescue, and the University of Adelaide. The University of Adelaide has financial interest in Sparc Hydrogen.

Acknowledgements

This work was supported by funding from The Australian Solar Thermal Research Initiative (ASTRI) program, which is supported by the Australian Government through the Australian Renewable Energy Agency (ARENA). TMR acknowledges funding support from ASTRI for a PhD scholarship. The authors also thank Sparc Hydrogen for additional support.

Notes and references

1 A. Fujishima and K. Honda, *Nature*, 1972, **238**, 37–38.
2 Q. Wang and K. Domen, *Chem. Rev.*, 2020, **120**, 919–985.
3 H. Nishiyama, T. Yamada, M. Nakabayashi, Y. Maehara, M. Yamaguchi, Y. Kuromiya, Y. Nagatsuma, H. Tokudome, S. Akiyama, T. Watanabe, R. Narushima, S. Okunaka, N. Shibata, T. Takata, T. Hisatomi and K. Domen, *Nature*, 2021, **598**, 304–307.
4 T. Hisatomi and K. Domen, *Nat. Catal.*, 2019, **2**, 387–399.
5 B. A. Pinaud, J. D. Benck, L. C. Seitz, A. J. Forman, Z. Chen, T. G. Deutsch, B. D. James, K. N. Baum, G. N. Baum, S. Ardo, H. Wang, E. Miller and T. F. Jaramillo, *Energy Environ. Sci.*, 2013, **6**, 1983–2002.
6 Q. Wang, C. Pornrungroj, S. Linley and E. Reisner, *Nat. Energy*, 2022, **7**, 13–24.
7 S. Chen, T. Takata and K. Domen, *Nat. Rev. Mater.*, 2017, **2**, 17050.
8 Y. Kageshima, H. Inuzuka, H. Kumagai, B. Ohtani, K. Teshima and H. Nishikiori, *J. Phys. Chem. C*, 2023, **127**, 18327–18339.
9 Y. Cho, A. Yamaguchi, R. Uehara, S. Yasuhara, T. Hoshina and M. Miyauchi, *J. Chem. Phys.*, 2020, **152**, 231101.
10 D. J. Kok, K. Irmscher, M. Naumann, C. Guguschev, Z. Galazka and R. Uecker, *Phys. Status Solidi A*, 2015, **212**, 1880–1887.
11 Y. Goto, T. Hisatomi, Q. Wang, T. Higashi, K. Ishikiriyama, T. Maeda, Y. Sakata, S. Okunaka, H. Tokudome, M. Katayama, S. Akiyama, H. Nishiyama, Y. Inoue, T. Takewaki, T. Setoyama, T. Minegishi, T. Takata, T. Yamada and K. Domen, *Joule*, 2018, **2**, 509–520.
12 C. K. N. Peh, M. Gao and G. W. Ho, *J. Mater. Chem. A*, 2015, **3**, 19360–19367.
13 A. Castedo, A. Casanovas, I. Angurell, L. Soler and J. Llorca, *Fuel*, 2018, **222**, 327–333.
14 P. Zhou, I. A. Navid, Y. Ma, Y. Xiao, P. Wang, Z. Ye, B. Zhou, K. Sun and Z. Mi, *Nature*, 2023, **613**, 66–70.
15 Y. Li, Y.-K. Peng, L. Hu, J. Zheng, D. Prabhakaran, S. Wu, T. J. Puchtler, M. Li, K.-Y. Wong, R. A. Taylor and S. C. E. Tsang, *Nat. Commun.*, 2019, **10**, 4421–4429.
16 K. Takanabe, *ACS Catal.*, 2017, **7**, 8006–8022.
17 T. Hisatomi, K. Maeda, K. Takanabe, J. Kubota and K. Domen, *J. Phys. Chem. C*, 2009, **113**, 21458–21466.
18 X. Zhu, D.-L. Chang, X.-S. Li, Z.-G. Sun, X.-Q. Deng and A.-M. Zhu, *Chem. Eng. J.*, 2015, **279**, 897–903.
19 S. Tabata, H. Ohnishi, E. Yagasaki, M. Ippommatsu and K. Domen, *Catal. Lett.*, 1994, **28**, 417–422.
20 Y. Deng, *Chem. Eng. J.*, 2018, **337**, 220–227.
21 T. Hisatomi, T. Minegishi and K. Domen, *Bull. Chem. Soc. Jpn.*, 2012, **85**, 647–655.
22 G. Rothenberger, J. Moser, M. Graetzel, N. Serpone and D. K. Sharma, *J. Am. Chem. Soc.*, 1985, **107**, 8054–8059.
23 J. Z. Bloh, *Front. Chem.*, 2019, **7**, 128.
24 T. Takata, J. Jiang, Y. Sakata, M. Nakabayashi, N. Shibata, V. Nandal, K. Seki, T. Hisatomi and K. Domen, *Nature*, 2020, **581**, 411–414.
25 Y. Ham, T. Hisatomi, Y. Goto, Y. Moriya, Y. Sakata, A. Yamakata, J. Kubota and K. Domen, *J. Mater. Chem. A*, 2016, **4**, 3027–3033.
26 J. F. Alvino, T. Bennett, R. Kler, R. J. Hudson, J. Aupoil, T. Nann, V. B. Golovko, G. G. Andersson and G. F. Metha, *Rev. Sci. Instrum.*, 2017, **88**, 054101.
27 G. Kim, H. J. Choi, H.-J. Kim, J. Kim, D. Monllor-Satoca, M. Kim and H. Park, *Photochem. Photobiol. Sci.*, 2016, **15**, 1247–1253.
28 X. Zhang, C. Xu, L. Zhang, Z. Li, J. Hong and Y. Zhang, *ACS Appl. Energy Mater.*, 2022, **5**, 4564–4576.
29 X. Li, J. Lin, J. Li, H. Zhang, X. Duan, H. Sun, Y. Huang, Y. Fang and S. Wang, *ACS Sustain. Chem. Eng.*, 2021, **9**, 7277–7285.

30 D. H. K. Murthy, V. Nandal, A. Furube, K. Seki, R. Katoh, H. Lyu, T. Hisatomi, K. Domen and H. Matsuzaki, *Adv. Energy Mater.*, 2023, **13**(40), 2302064.
31 A. V. Bandura and S. N. Lvov, *J. Phys. Chem. Ref. Data*, 2006, **35**, 15–30.
32 T. Liu, P. Wang, W. Li, D. Z. Wang, D. D. Lekamge, B. Chen, F. A. Houle, M. M. Waegele and D. Wang, *ACS Cent. Sci.*, 2024, **11**, 91–97.